Contributed paper

OPTO-ELECTRONICS REVIEW 7(4), 369–374 (1999)

Characteristics of infrared photodiode using SiO_2 insulator on InSb wafer with p-i-n structure

J.Y. CHO*, J.S. KIM, S.H. SON, J.H. LEE, and S.Y. CHOI

Department of Electrical Engineering, Kyungpook National University
Taegu, 702–701, Korea

A highly sensitive photovoltaic infrared diode was fabricated for detecting a 3–5 μm wavelength range in an InSb wafer with a p-i-n structure grown by MOCVD. The formation of silicon dioxide (SiO_2) insulator films for the junction interface and surface of the photodiode were prepared using remote plasma enhanced chemical vapour deposition (PECVD) as InSb has a low melting point and evaporation temperature for surface atoms. The structural characteristics of SiO_2 films and electrical characteristics of metal-insulator-semiconductor structures were initially examined. The leakage current density at 1 MV/cm was about 22 nA/cm^2, the breakdown electric field of the MIS capacitor using SiO_2 film deposited at 105°C was about 3.5 MV/cm, and the interface-state density at the mid-band gap extracted from the 1 MHz capacitance-voltage measurement was about 2×10^{11} cm^{-2}eV^{-1}. Thereafter, the characteristics of the infrared photodiode were examined. The product of zero-bias resistance by area (R_0A) showed 1.56×10^6 Ω cm^2 and normalized detectivity exhibited about 1×10^{11} cmHz$^{1/2}$W^{-1}.

Keywords: InSb photodiodes, InSb MIS structure, SiO_2 insulator film, C-V characteristics.

1. Introduction

All materials with thermal energy sources eject infrared with differing wavelengths according to temperature. The infrared wavelength ranges ejected by high thermal energy sources, like a missile, are 3–5 μm. Since these ranges correspond to the minimum absorption range of air, a semiconductor material with a corresponding energy-gap can detect infrared [1].

Among the many III–V compound semiconductors, InSb is widely used in infrared imaging systems [2,3]. Dielectric layers that possess good insulating and interfacial properties are essential for the effective performance of large and dense focal plane arrays. However, the relatively low melting point of InSb leads to a deviation in the stoichiometry of its surface layers at elevated temperatures. It has been reported that substantial amounts of oxidation or incongruent evaporation occur at temperatures above 250°C [4,5]. Accordingly, low temperature techniques are necessary for the formation of insulators on InSb. The remote plasma enhanced chemical vapour deposition (PECVD) process has been used

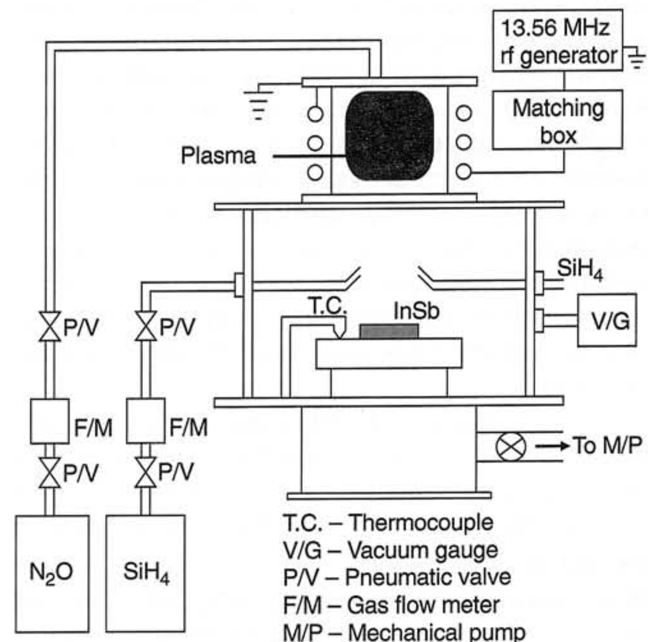

Fig. 1. Schematic diagram of a remote PECVD reactor.

*e-mail: heaven5@palgong.kyungpook.ac.kr

for the formation of SiO_2. In remote PECVD only some of the process gases are subjected to direct plasma excitation and the substrate is outside of the plasma glow region [6]. Consequently, impurities can be minimized by adjusting reaction pathways to avoid unwanted chemical reactions and the effects of bombardment. This alleviates the serious problems encountered in the direct PECVD process.

The purpose of this research, therefore, is to study both the formation of high-quality SiO_2 films on InSb using the low temperature remote PECVD technique and the fabrication of an infrared photodiodes. The effects of deposition parameters on the structural characteristics of SiO_2 films and the electrical properties of MIS structures were initially investigated. Thereafter, the characteristics of an infrared diodes, fabricated using an InSb wafer with a p-i-n structure, were identified.

2. Experiments

2.1. Formation of silicon dioxide (SiO_2) films

High quality surface passivation is necessary for InSb photodiodes. However, the formation of surface passivation films by sputtering can transform the properties of the material due to surface damage, accordingly, low-temperature remote PECVD was used.

The configuration of a remote PECVD reactor is shown schematically in Fig. 1. The diameters of the quartz plasma excitation tube and stainless steel deposition chamber were 110 and 320 mm, respectively. N_2O was introduced into the quartz tube, which was inductively coupled to a 13.56 MHz RF source, to produce activated oxygen radicals. SiH_4 (10% diluted in Ar) was introduced into the deposition chamber through an injection nozzle positioned 100 mm below the point at which the plasma generation tube entered the deposition chamber, and the deposition substrate was positioned 100 mm below the injection nozzle.

The substrates used in this study were (100) oriented, n-type, single crystal InSb, doped by Te within a concentration range of $(3.5–6.0)\times10^{14}$ cm^{-3} at 77 K. The thickness of the SiO_2 films on the InSb for use in the MIS capacitors was 1300 Å. Ohmic back contacts were obtained by evaporating In, and the gate electrodes were formed by the selective evaporation of Ni.

2.2. Fabrication of InSb photodiode

The InSb wafer used in this study was n–type InSb doped by Te, and the n^- and p^+ layers were then grown by MOCVD on this n^-–type InSb wafer. The concentration of the p^+ layer was 2×10^{18} cm^{-3} and the thickness was 0.75 μm. The n^-–layer was an undoped layer with a 1.5 μm thickness. The area of the infrared sensor was 7×5 mm^2 and that of the p^+ –layer, which etched the unit cell mesa in the sensor, was 300×700 μm^2.

Table 1. Process sequence for the fabrication of infrared diode

Process sequence	Conditions
1. Initial Cleaning	
2. Mesa etching	HF : H_2O_2 : H_2O = 1:1:80
3. Surface preparation before SiO_2 deposition	NH_4OH : H_2O_2, HCl : H_2O
4. SiO_2 deposition	Using remote PECVD
5. Contact open	HF : H_2O = 1:50
6. Metal deposition	Evaporation using In and Au
7. Wire bonding	

Table 1 illustrates the fabrication sequence of the infrared diode. For satisfying the condition of anti-reflecting (AR) coating, SiO_2 films of about 5000 Å were deposited. Figure 2 schematically outlines a cross-sectional view of the infrared diode. Ohmic contacts were obtained by evaporating about 2000 Å of In.

3. Results and discussion

The growth rate and refractive index have a critical dependence on many parameters including the gas flow ratio of reactant gases, substrate temperature, RF input power, and deposition pressure. Figure 3 shows

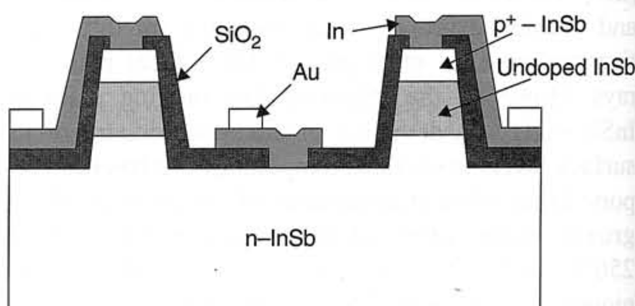

Fig. 2. Cross sectional view of infrared diode.

 © 1999 COSiW SEP, Warsaw

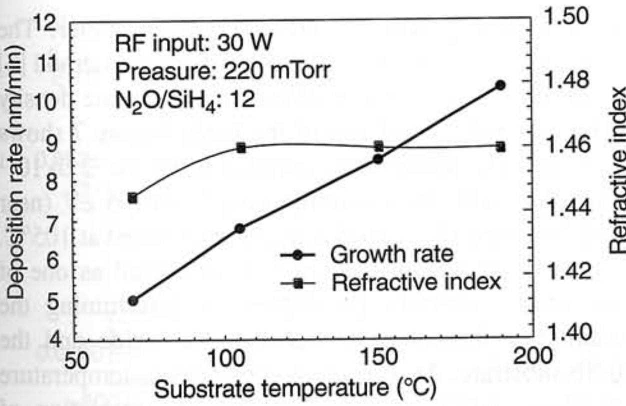

Fig. 3. Deposition rate and refractive index of silicon oxide films deposited by PECVD in relation to the deposition temperature.

the linear relationship of the growth rate and refractive index of silicon oxide films in relation to the substrate temperature. From this graph, we could determine the minimum substrate temperature. The refractive index indicates a constant value of 1.46 for films deposited at 105°C and above. The activation energy was calculated to be 0.01 eV.

The relation between the deposition rate and gas flow ratio (N_2O/SiH_4) for silicon oxide films is shown in Fig. 4. According to a previous report [7], the growth rate curve in Fig. 4 can be divided into "reaction rate controlled" and "retardation controlled" regimes for low and high N_2O flow rates, respectively.

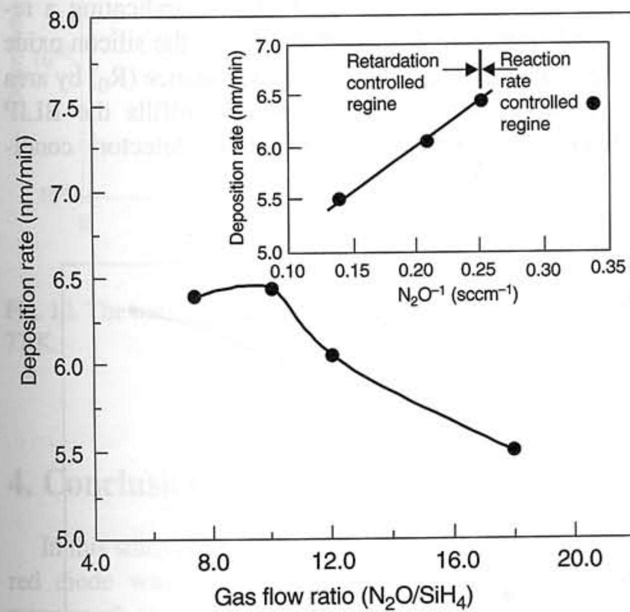

Fig. 4. Deposition rate of silicon oxide films as a function of reactant gas flow ratio (N_2O/SiH_4). The inserted figure shows the linear variation of the deposition rate with a reciprocal N_2O flow rate (retardation controlled regime).

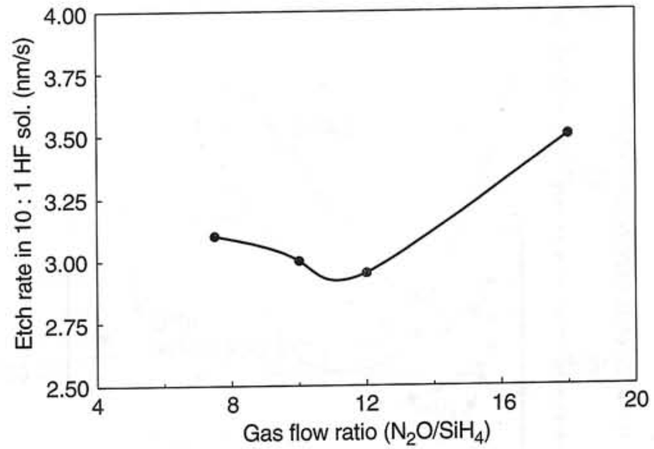

Fig. 5. Etching rate in a solution consisting of 1 part 48% HF and 10 parts deionized water for the samples shown in Fig. 4.

This retardation theory may explain the similar results found for low-temperature CVD and the reduced deposition rates with high N_2O/SiH_4 ratios. The deposition process involves the incidence of the reactant on the surface of molecules plus the simultaneous evaporation of some of the previously deposited molecules. The retardation theory explains that the surface reaction rate is inversely proportional to the strength of the concentration of gas held on the surface, thereby, producing retardation with a reactant. The linear variation of the deposition rate with a reciprocal N_2O flow rate is plotted in the inset in Fig. 4, and supports this theory.

The composition of the film was found to depend upon the conditions corresponding to the regimes in which the deposition occurred was achieved. Figure 5 shows the etch rate of oxide films deposited at various N_2O/SiH_4 ratios. The films deposited at a N_2O/SiH_4 ratio of around 12 indicated the highest density, whereas films deposited at ratios higher or lower than 12 indicated a lower density. It could be

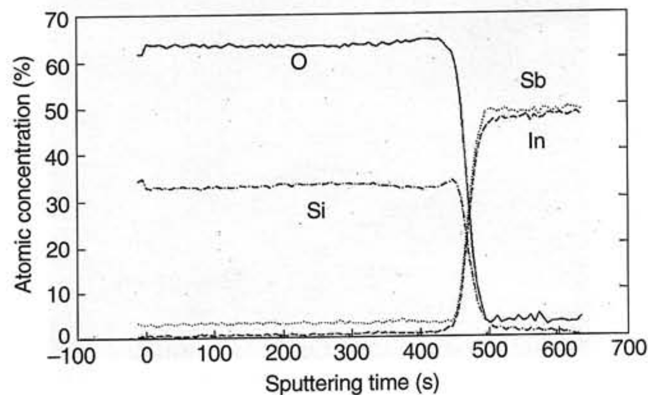

Fig. 6. AES depth profile of SiO_2 film deposited at 105°C.

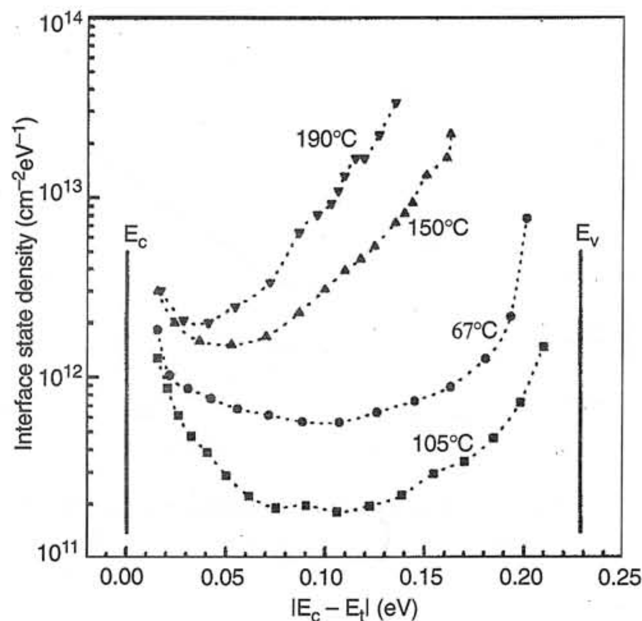

Fig. 7. Interface state density distributions of MIS capacitors using SiO_2 deposited at several substrate temperatures.

suggested that the films deposited at lower ratios were silicon-rich films while the films deposited at higher ratios contained SiO_x powders that were formed in the gas phase.

Figure 6 shows the AES measurements for SiO_2 films, deposited at 105°C with a N_2O to SiH_4 flow ratio of 12, recorded at different depths during Ar^+ (1.5 keV) sputtering. No significant concentrations of In or Sb were detected in the bulk of the SiO_2 indicating that negligible out diffusion of In or Sb atoms from the InSb surface took place during the SiO_2 deposition.

The C-V curves of the MIS capacitors deposited on the SiO_2 films at different deposition temperatures were measured using a HP4280A C-V meter. The C-V curve was analyzed using the Terman method [8] to obtain the distribution of the interface state density (D_{it}) across the band gap of the InSb. Figure 7 shows that the D_{it} value was estimated to be 2.0×10^{11} $cm^{-2}eV^{-1}$ with the minimum near E_t–0.105 eV (near mid-band gap) for a MIS capacitor prepared at 105°C. The deposition temperature was identified as one of the most important parameters in determining the quality of the interface between the oxide and the InSb substrate. As a result, a compromise temperature of about 100°C is suggested for the formation of high-quality remote PECVD SiO_2 films on InSb.

Figure 8(a) shows the cross-sectional view of an InSb surface after mesa etching using HF: H_2O_2 : H_2O = 1:1:80. The angle of the mesa-etching surface was about 70° which can be used for the uniform deposit of SiO_2 for the passivation of any surface leakage current. Figure 8(b) shows the etching rate of InSb using a mesa etching solution and the etched depth was measured using α-step.

The I-V curve at 77 K of the fabricated infrared diode was measured using an HP4145B semiconductor parameter analyser. Figure 9 shows the I-V curves of the fotodiode before and after silicon oxide films were deposited on an InSb wafer with a p-i-n structure. Figure 9(a) indicates about 650 μA with a reverse voltage (500 mV) because of the increased surface leakage current due to undeposited SiO_2. However, Fig. 9(b) shows the nA scales of leakage current with a reverse voltage of 500 mV, indicating a reduced surface leakage current due to the silicon oxide films. The product of zero-bias resistance (R_0) by area (A) was 1.56×10^6 $\Omega\,cm^2$, which fulfills the BLIP (background limited infrared photodetector) conditions.

(a)

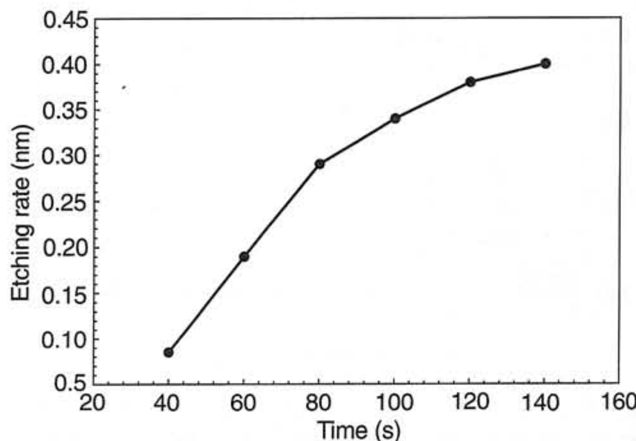

(b)

Fig. 8. Cross-sectional view of InSb surface after mesa etching (a), eching rate at 40°C (b).

 © 1999 COSiW SEP, Warsaw

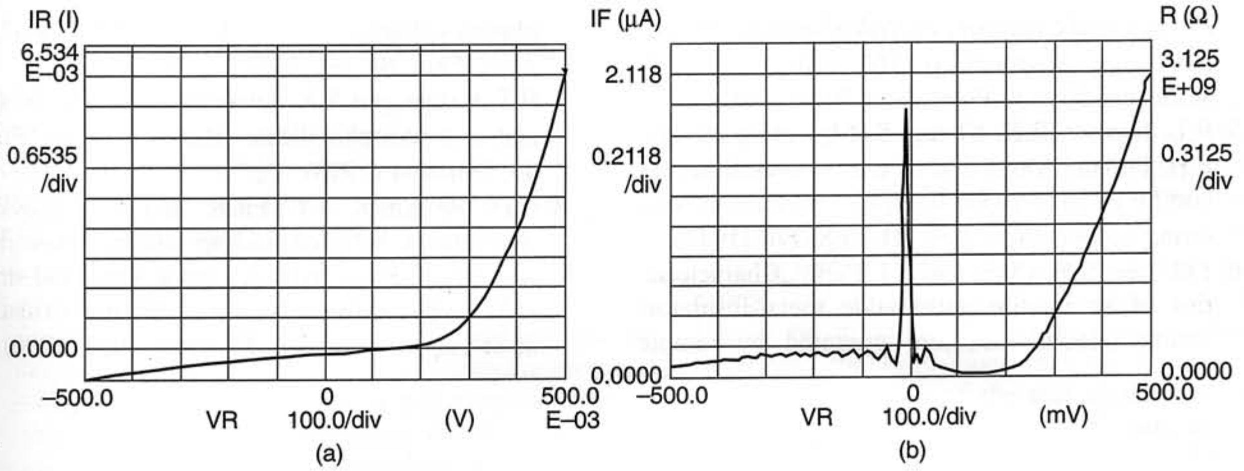

Fig. 9. The I-V characteristics of diode before and after cleaning and SiO_2 deposition at 77 K: (a) before (IR = Current , VR = Voltage), (b) after (IF = Current , VF = Voltage).

The results of normalised detectivity with various injected infrared wavelength ranges are shown in Fig. 10. As expected, the InSb infrared diode exhibited high normalized detectivity, 1×10^{11} $cmHz^{1/2}W^{-1}$, within a 3–5 µm range.

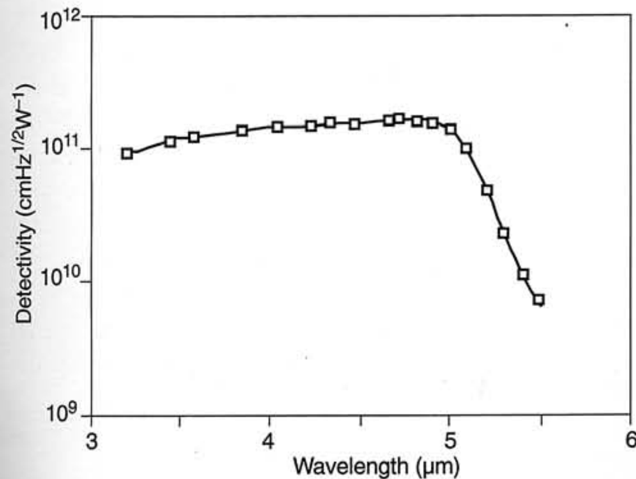

Fig. 10. The normalized detectivity of InSb photodiodes at 77 K.

4. Conclusions

In this study, a highly-sensitive photovoltaic infrared diode was fabricated for detecting a 3–5 µm wavelength range in an InSb wafer with a p-i-n structure grown by MOCVD.

A low-temperature remote PECVD technique was developed for the formation of high-quality SiO_2 films on InSb. The effects of deposition parameters, such as substrate temperature and gas-flow ratio, on the structural characteristics of SiO_2 films plus the electrical properties of MIS structures were studied. The density of SiO_2 films significantly decreased with high pressure and high N_2O/SiH_4 gas flow ratio ranges. This is probably due to gas phase nucleation promoted by gas phase collisions. InSb MIS capacitors were fabricated using SiO_2 films deposited within a temperature range of 67–190°C. The interface-state density at the mid-band gap of the MIS capacitor was about 2.0×10^{11} $cm^{-2}eV^{-1}$ when the SiO_2 film was deposited at 105°C.

The I-V curve of the fabricated infrared diode was measured at 77 K. The value of R_0A product was 1.56×10^{6} $\Omega\,cm^2$, which satisfies BLIP conditions. The InSb infrared diode exhibited high normalized detectivity, 1×10^{11} $cmHz^{1/2}W^{-1}$ within a 3–5 µm range. Accordingly, this good quantum efficiency and high detectivity will permit use of InSb photodiode as a unit cell in an array.

References

1. E.H. Putley, "Indium antimonide submillimeter photoconductive detectors", *Appl. Opt.* **4**, 649–656 (1965).
2. R.D. Thom, T.L. Koch, J.D. Langan, and W.J. Parrish, "A fully monolithic InSb infrared CCD array", *IEEE Trans. Electron Devices* **ED-27**, 160–170 (1980).
3. S.R. Kurtz, R.M. Biefeld, L.R. Dawson, I.J. Fritz, and T.E. Zipperian, "High photoconductive gain in lateral InAsSb strained-layer superlattice infrared detectors," *Appl. Phys. Lett.* **53**, 1961–1963 (1988).
4. J.F. Wager and C.W. Wilmsen, "The deposited insulator/III-V semiconductor interface," in

Physics and Chemistry of III-V Compound Semiconductor Interfaces, p. 168, edited by C.W. Wilmsen, Plenum Press, New York, 1985.
5. R.L. Farrow, R.K. Chang, S. Mroczkowski, and F.H. Pollak, "Detection of excess crystalline As and Sb in III-V oxide interfaces by Raman scattering", *Appl. Phys. Lett.* **31**, 768–770 (1977).
6. J.G. Lee, S.Y. Choi, and S.J. Park, „Characteristics of an indium antimonide metal-insulator-semiconductor structure prepared by remote plasma enhanced chemical vapor deposition", *J. Appl. Phys.* **82**, 3917–1921 (1997).
7. B.J. Baliga and S.K. Ghandhi, „Growth of silicon and phosphosilicate films", *J. Appl. Phys.* **44**, 990–994 (1973).
8. C.H. Bjorkman, J.T. Fitch, and G. Lucovsky, „Correlation between midgap interface state density and thickness-averaged oxide stress and strain at Si/SiO_2 interfaces formed by thermal oxidation of Si", *Appl. Phys. Lett.* **56**, 1983–1985 (1990).

 © 1999 COSiW SEP, Warsaw